Spatial Shape of Electron Delocalization: Structure of the Laplacian of the Negative Exchange−Correlation Density

Jens Geier†

Bergische Universität Wuppertal, FB C-Anorganische Chemie, Gaussstrasse 20, D-42097 Wuppertal, Germany

Received: March 10, 2006; In Final Form: May 9, 2006

The Laplacian of the negative exchange−correlation density (with respect to coordinate $\mathbf{r}_2$), $\nabla_{\langle \mathbf{r}_2 \rangle}^2[-\Gamma_{XC}^{\sigma_1\sigma_2}(\mathbf{r}_1,\mathbf{r}_2)] = \nabla_{\langle \mathbf{r}_2 \rangle}^2 X^{\sigma_1\sigma_2}(\mathbf{r}_1,\mathbf{r}_2)$, is proposed as an instrument for the analysis of electron delocalization in real space. It determines local concentrations in the amount of electrons that are delocalized from a reference point $\mathbf{r}_1$ over space. Integration of the reference coordinate $\mathbf{r}_1$ over an atomic basin Ω_n gives the function $\nabla^2 X^{\sigma_1\sigma_2}(\Omega_n;\mathbf{r})$, which contains detailed information about the spatial shape of the delocalization that originates from an atom in a molecule. Its isosurface representations are richly structured and resemble molecular orbitals in their complexity and partly also in their shape. The sum over all $\nabla^2 X^{\sigma_1\sigma_2}(\Omega_n;\mathbf{r})$ functions of a molecule equals the Laplacian of the electron density $\nabla^2\rho(\mathbf{r})$, for which it provides a meaningful partitioning into atomic contributions.

Introduction

Functions such as the electron density $\rho(\mathbf{r})$,[1,2] its Laplacian $\nabla^2\rho(\mathbf{r})$,[3−6] or the electron localization function (ELF) $\eta(\mathbf{r})$[7−9] enable the description of electronic structures in real space. The topological analysis of $\rho(\mathbf{r})$ provides quantum mechanically exactly defined atomic basins, which are nonoverlapping volumes in real space, each one associated with an electron density maximum.[1,2] Moreover, the presence of bonding between two atoms is indicated by the occurrence of (3, −1) critical points in $\rho(\mathbf{r})$.[10] Finer details, like the atomic shell structure or the presence of nonbonded domains (corresponding to the concept of the lone pair), are revealed by its Laplacian $\nabla^2\rho(\mathbf{r})$, which has the property of determining local concentrations ($\nabla^2\rho(\mathbf{r}) < 0$) and depletions ($\nabla^2\rho(\mathbf{r}) > 0$) in $\rho(\mathbf{r})$. The ELF $\eta(\mathbf{r})$, which can be related to the local spin pair composition,[11] resembles $\nabla^2\rho(\mathbf{r})$ in many respects[5] but is occasionally more easy to interpret in chemical terms.

Some of the most important concepts in chemistry, like those of electron delocalization[12] and electron pairing,[5,13] are associated with nonlocal electronic properties. Their description requires, therefore, functions with dependence on more than one space-spin coordinate (the latter are denoted by numbers, e.g., $1 = \mathbf{r}_1 s_1$). This work concerns the spatial shape of the electron delocalization that arises from certain points or volumes within molecules. Although electron delocalization is most frequently discussed in terms of molecular orbitals, there are also examples for its description in real space, which are related to the exchange−correlation density (vide infra). It will be demonstrated here that the Laplacian of the latter (whose structure was not investigated so far) is very well suited for this purpose and affords remarkably clear visualizations of even subtle details in electronic structures.

1. Theory

The electron pair density $\Gamma(1,2)$ is the diagonal element of the second-order reduced density matrix $\Gamma(1,2;1',2')$. The latter is formed from the N-electron density matrix by integration over all but two space-spin coordinates:[14,15]

$$\Gamma(1,2;1',2') = \frac{1}{2}N(N-1)\int \mathrm{d}3, \ldots, \mathrm{d}N\, \Psi(1,2,3,\ldots,N)\cdot \Psi^*(1',2',3,\ldots,N) \quad (1)$$

$\Gamma(1,2)$ can be written as sum of the uncorrelated product of electron densities and the exchange−correlation density $\Gamma_{XC}(1,2)$:[16]

$$\Gamma(1,2) = \frac{1}{2}[\rho(1)\,\rho(2) + \Gamma_{XC}(1,2)] \quad (2)$$

$\Gamma(1,2)\,\mathrm{d}v_1\,\mathrm{d}v_2$ is the probability of finding an electron within the volume $\mathrm{d}v_1$ around $\mathbf{r}_1$ with spin s_1 and another one within the volume $\mathrm{d}v_2$ around $\mathbf{r}_2$ with spin s_2. $\Gamma(1,2)$ is normalized to the number of distinct electron pairs, which can be formed from N electrons: $1/2\cdot N(N-1)$.[17] Integration over the spin coordinates partitions $\Gamma(1,2)$ into four components

$$\Gamma(\mathbf{r}_1,\mathbf{r}_2) = \int \mathrm{d}s_1\,\mathrm{d}s_2\,\Gamma(\mathbf{r}_1 s_1,\mathbf{r}_2 s_2) = \Gamma^{\alpha\alpha}(\mathbf{r}_1,\mathbf{r}_2) + \Gamma^{\alpha\beta}(\mathbf{r}_1,\mathbf{r}_2) + \Gamma^{\beta\alpha}(\mathbf{r}_1,\mathbf{r}_2) + \Gamma^{\beta\beta}(\mathbf{r}_1,\mathbf{r}_2) \quad (3)$$

with

$$\Gamma^{\sigma_1\sigma_2}(\mathbf{r}_1,\mathbf{r}_2) = \frac{1}{2}\cdot[\rho^{\sigma_1}(\mathbf{r}_1)\,\rho^{\sigma_2}(\mathbf{r}_2) + \Gamma_{XC}^{\sigma_1\sigma_2}(\mathbf{r}_1,\mathbf{r}_2)] \quad (4)$$

(σ_i denotes the spin state).

Due to electron delocalization between $\mathbf{r}_1$ and $\mathbf{r}_2$, the uncorrelated product of the electron densities at these points contains fictitious self-pairings, which are removed by the (negative) exchange parts of $\Gamma_{XC}^{\alpha\alpha}(\mathbf{r}_1,\mathbf{r}_2)$ and $\Gamma_{XC}^{\beta\beta}(\mathbf{r}_1,\mathbf{r}_2)$, respectively.[18] In addition to the dominating exchange, which describes the electron correlation that arises from the antisymmetry condition of the Pauli principle (Fermi correlation), $\Gamma_{XC}(\mathbf{r}_1,\mathbf{r}_2)$

† E-mail: geier@uni-wuppertal.de.

10.1021/jp061498f CCC: $33.50
Published on Web 07/06/2006

also contains the effects of Coulomb correlation. The latter is present for all components of $\Gamma_{XC}(\mathbf{r}_1,\mathbf{r}_2)$; in the case of the unlike-spin components $\Gamma_{XC}^{\alpha\beta}(\mathbf{r}_1,\mathbf{r}_2)$ and $\Gamma_{XC}^{\beta\alpha}(\mathbf{r}_1,\mathbf{r}_2)$, it is the single source of correlation.[16,18,19] The spin-integrated exchange−correlation density $\Gamma_{XC}(\mathbf{r}_1,\mathbf{r}_2)$ is a quantitative measure of the electron delocalization from a reference point $\mathbf{r}_1$ over the point $\mathbf{r}_2$ in real space.[12,18−28] The magnitude of its integral over $\mathbf{r}_2$ thus equals the electron density at $\mathbf{r}_1$ (and vice versa):

$$\int d\mathbf{r}_2\, \Gamma_{XC}(\mathbf{r}_1,\mathbf{r}_2) = \int d\mathbf{r}_2\, \Gamma_{XC}^{\alpha\alpha}(\mathbf{r}_1,\mathbf{r}_2) + \int d\mathbf{r}_2\, \Gamma_{XC}^{\alpha\beta}(\mathbf{r}_1,\mathbf{r}_2) + \int d\mathbf{r}_2\, \Gamma_{XC}^{\beta\alpha}(\mathbf{r}_1,\mathbf{r}_2) + \int d\mathbf{r}_2\, \Gamma_{XC}^{\beta\beta}(\mathbf{r}_1,\mathbf{r}_2) = -\rho^{\alpha}(\mathbf{r}_1) + 2\cdot 0 - \rho^{\beta}(\mathbf{r}_1) = -\rho(\mathbf{r}_1) \quad (5)$$

Its integration, with respect to $\mathbf{r}_1$ and $\mathbf{r}_2$, over atomic basins[1,2] gives, after sign inversion, the number of electrons which are localized in a particular basin (the localization index) or delocalized from one atom over another ($=^1/_2$ times the delocalization index).[18−26] The sharing index $I(\zeta,\zeta')$, which approximates $-\Gamma_{XC}(\mathbf{r}_1,\mathbf{r}_2)$ and equals it at the Hartree−Fock level, was derived solely from the first-order reduced density matrix without use of the electron pair density.[29−31] Because $\Gamma_{XC}(\mathbf{r}_1,\mathbf{r}_2)$, defined by eq 2, is generally negative, i.e., small values correspond to pronounced delocalization and vice versa, it will be used with inverted sign, under the name $X(\mathbf{r}_1,\mathbf{r}_2)$, throughout this paper:

$$X(\mathbf{r}_1,\mathbf{r}_2) = -\Gamma_{XC}(\mathbf{r}_1,\mathbf{r}_2) \quad (6)$$

The evaluation of $X(\mathbf{r}_1,\mathbf{r}_2)$ along coordinate $\mathbf{r}_2$ for a fixed reference point $\mathbf{r}_1$ (or volume Ω_1) reveals a rich structure, which becomes, however, increasingly uniform the more the reference point is spatially approached by $\mathbf{r}_2$. Delocalization in the vicinity of the reference point is so extensive that $X(\mathbf{r}_1,\mathbf{r}_2)$ already resembles $\rho(\mathbf{r})$ in this region. The strong contrast-enhancing effect of the Laplace operator on $\rho(\mathbf{r})$ suggests its application with respect to $\mathbf{r}_2$ (indicated by the subscript $\langle\mathbf{r}_2\rangle$) on $X(\mathbf{r}_1,\mathbf{r}_2)$. The resulting function $\nabla_{\langle\mathbf{r}_2\rangle}^2 X(\mathbf{r}_1,\mathbf{r}_2)$, which determines local concentrations and depletions (vide supra) in the amount of electrons that are delocalized from $\mathbf{r}_1$ over space, is expected to provide more clear-cut representations of the basic structure of electron delocalization. It will be shown that it enables also a meaningful partitioning of the well-known Laplacian of the electron density, $\nabla^2\rho(\mathbf{r})$, into atomic contributions.

The Hartree−Fock (HF) second-order reduced density matrix $\Gamma(1,2;1',2')$ is entirely determined by the corresponding first-order reduced density matrix (γ):[14,15]

$$\Gamma(1,2;1',2') = \frac{1}{2}[\gamma(1,1')\,\gamma(2,2') - \gamma(2,1')\,\gamma(1,2')] \quad (7)$$

It includes exchange, but no Coulomb correlation; hence $\Gamma_{XC}(1,2)$ reduces to a pure exchange density $\Gamma_X(1,2)$, which is given, after spin integration, in terms of molecular spin−orbitals $\varphi_i(\mathbf{r})$ by

$$\Gamma_X(\mathbf{r}_1,\mathbf{r}_2) = \Gamma_X^{\alpha\alpha}(\mathbf{r}_1,\mathbf{r}_2) + \Gamma_X^{\beta\beta}(\mathbf{r}_1,\mathbf{r}_2) = -\sum_i\sum_j \varphi^*_{i,\alpha}(\mathbf{r}_1)\,\varphi_{j,\alpha}(\mathbf{r}_1)\,\varphi^*_{j,\alpha}(\mathbf{r}_2)\,\varphi_{i,\alpha}(\mathbf{r}_2) - \sum_i\sum_j \varphi^*_{i,\beta}(\mathbf{r}_1)\,\varphi_{j,\beta}(\mathbf{r}_1)\,\varphi^*_{j,\beta}(\mathbf{r}_2)\,\varphi_{i,\beta}(\mathbf{r}_2) \quad (8)$$

where the sums run over the occupied orbitals only. It has been demonstrated that this expression is also meaningful with the Kohn−Sham orbitals obtained from DFT calculations, when the B3LYP[32−35] hybrid functional is used.[36,37] Compared to HF theory, the B3LYP method leads to slightly stronger electron delocalization.[19] In this work, B3LYP orbitals are used instead of HF orbitals for the calculation of the exchange(−correlation) density, to perform molecular geometry optimizations and the analysis of electronic structures, which involves also the evaluation of properties of the electron density, at the same theoretical level (molecular structures and electron densities obtained from B3LYP are superior to those from HF). Inclusion of Coulomb correlation by means of post-HF methods lowers the extent of delocalization.[19] The analysis of exact pair densities has been described for CI[18,19] and SC[25] calculations, but at the moment the explicit calculation of $\Gamma_{XC}(\mathbf{r}_1,\mathbf{r}_2)$ at post-HF levels is practically limited, because pair densities are yet not readily available for many of the correlated methods. In such cases the exchange−correlation density may be approximated by the following expression,[16,21] where $\varphi_i(\mathbf{r})$ are natural spin−orbitals and ν_i are their occupation numbers (except for the sign, it is identical with the sharing index[29−31]):

$$\tilde{\Gamma}_{XC}(\mathbf{r}_1,\mathbf{r}_2) = \Gamma_{XC}^{\alpha(\alpha+\beta)}(\mathbf{r}_1,\mathbf{r}_2) + \Gamma_{XC}^{\beta(\beta+\alpha)}(\mathbf{r}_1,\mathbf{r}_2) = -\sum_i\sum_j \nu_i^{1/2}\nu_j^{1/2}\varphi^*_{i,\alpha}(\mathbf{r}_1)\,\varphi_{j,\alpha}(\mathbf{r}_1)\varphi^*_{j,\alpha}(\mathbf{r}_2)\,\varphi_{i,\alpha}(\mathbf{r}_2) - \sum_i\sum_j \nu_i^{1/2}\nu_j^{1/2}\varphi^*_{i,\beta}(\mathbf{r}_1)\,\varphi_{j,\beta}(\mathbf{r}_1)\,\varphi^*_{j,\beta}(\mathbf{r}_2)\,\varphi_{i,\beta}(\mathbf{r}_2) = -\tilde{X}(\mathbf{r}_1,\mathbf{r}_2) \quad (9)$$

In the case of $\nu_i = 1$ for all i (i.e., in single determinant calculations) it is identical with the HF expression. The required natural orbitals and occupation numbers can be obtained for several post-HF methods, including MP2, QCISD and CCSD, with popular quantum-chemical software.

Integration of the exchange−correlation density $\Gamma_{XC}(\mathbf{r}_1,\mathbf{r}_2)$ with respect to $\mathbf{r}_1$ over the volume Ω_n of atom n (defined by QTAIM, i.e., the topological analysis of the electron density[1,2]) and renaming coordinate $\mathbf{r}_2$ to $\mathbf{r}$ gives the atomic exchange−correlation density $\Gamma_{XC}(\Omega_n;\mathbf{r})$,[38,39] which is, after sign inversion, also called the domain-averaged Fermi hole:[27,28,40−43]

$$\Gamma_{XC}(\Omega_n;\mathbf{r}) = -X(\Omega_n;\mathbf{r}) = \int_{\Omega_n} d\mathbf{r}_1\, \Gamma_{XC}(\mathbf{r}_1,\mathbf{r}_2)|_{\mathbf{r}_2=\mathbf{r}} \quad (10)$$

It describes how the electron population of an atom in a molecule is delocalized over space. A special method of extracting information from this function starts with its matrix representation and involves diagonalization and subsequent isopycnic transformation of the eigenvectors.[27,28,40−43] Depending on their spatial shape and the associated eigenvalues, the latter can be related to chemical objects and terms such as core electrons, bonded or nonbonded electron pairs and free valences of molecular subunits.

In the above approximation (eq 9, which is exact at the HF level) $\Gamma_{XC}(\Omega_n;\mathbf{r})$ equals the negative volume-point sharing index[29−31] and is given by

$$\tilde{\Gamma}_{XC}(\Omega_n;\mathbf{r}) = -\sum_i\sum_j \nu_i^{1/2}\nu_j^{1/2} S[\Omega_n]_{ij}^{\alpha}\varphi_{i,\alpha}(\mathbf{r})\varphi^*_{j,\alpha}(\mathbf{r}) - \sum_i\sum_j \nu_i^{1/2}\nu_j^{1/2} S[\Omega_n]_{ij}^{\beta}\varphi_{i,\beta}(\mathbf{r})\varphi^*_{j,\beta}(\mathbf{r}) = -\tilde{X}(\Omega_n;\mathbf{r}) \quad (11)$$

where $S[\Omega_n]_{ij}$ are elements of the atomic overlap matrix[18] with respect to Ω_n (i.e., the integrals of the orbital products $\varphi_i(\mathbf{r})\varphi_j(\mathbf{r})$ over the basin Ω_n). Because the division of molecular space into QTAIM basins is disjoint (i.e nonoverlapping and complete), summation of all $X(\Omega_n;\mathbf{r})$ functions for a molecule

is equal to the integration of $X(\mathbf{r}_1,\mathbf{r}_2)$ over $\mathbf{r}_1$ and hence gives the electron density at $\mathbf{r}$ (cf. eq 5). Correspondingly, the sum of all $\nabla^2X(\Omega_n;\mathbf{r})$ functions for a molecule equals the Laplacian of the electron density:

$$\nabla^2\rho(\mathbf{r}) = \sum_n \nabla^2X(\Omega_n;\mathbf{r}) \tag{12}$$

The structure of $\nabla^2\rho(\mathbf{r})$ is related to the extent of electron localization (partial pair condensation[3]) in the vicinity of a point $\mathbf{r}$, and therefore also to the local concentration of the exchange−correlation density around this point as reference ($\mathbf{r}_1 = \mathbf{r}$). The $\nabla^2X(\Omega_n;\mathbf{r})$ functions represent hence a meaningful decomposition of $\nabla^2\rho(\mathbf{r})$ into atomic contributions. They provide a connection between the direction of the electron delocalization that arises from a particular atomic basin and the spatial location of the remaining electrons. In contrast to molecular orbitals, the exchange−correlation density and its Laplacian are invariant to unitary transformations and are, therefore, like $\rho(\mathbf{r})$, $\nabla^2\rho(\mathbf{r})$, $\eta(\mathbf{r})$ and $I(\zeta,\zeta')$, unambiguous instruments for extracting information from wave functions.

2. Computational Details

The structures of molecules **1**−**8** and **10** were optimized with the *Gaussian 03* program package[44] at the B3LYP/6-311++G(2d,2p) level,[32−35] starting with RHF/6-311++G(2d,2p) orbitals as the initial guess. Cartesian d functions were used throughout. Unless otherwise stated, all structures are minima according to their Hessian eigenvalues. The validity of the single reference calculations was checked in all cases by a stability analysis.[45] Molecule **9** was optimized with the UCCSD/6-31+G(d) method.[46] The B3LYP orbitals or natural orbitals, respectively, and their occupation numbers were written to *wfn* output files by means of the Keywords: 6d, DENSITY=CURRENT (for B3LYP) or DENSITY=CC (for CCSD), OUTPUT=WFN. Separate α- and β-orbitals were obtained with the additional Keyword POP=NOAB.

The topological analysis of the electron density was performed with the program *AIM2000*,[47] which uses the *wfn* files as input (in the case of separate α- and β-orbitals these were both contained in a single *wfn* file). The integrations over atomic basins were done in natural coordinates with relative and absolute accuracies of 10^{-6} (with exception of compound **3**, where these values both had to be increased to 10^{-5}). The magnitudes of the integrals of $L(\mathbf{r}) = -{}^1/_4\nabla^2\rho(\mathbf{r})$ were smaller than 10^{-3} au in all cases. The atomic overlap matrix was obtained from the integration record file.

A *Fortran* program[48] was written, which uses these record files and the *wfn* files as input for the calculation of the exchange−correlation density and its Laplacian over a cubic grid, according to eqs 9 and 11. The grid values were evaluated in steps ranging from 0.10 to 0.15 au and were saved in *cube* format. Graphical representations were generated from the *cube* files with the program *Molekel*.[49,50] ELF grids were calculated with the program package *ToPMod*.[51]

3. Results and Discussion

$X(\Omega_n;\mathbf{r})$ and $\nabla^2X(\Omega_n;\mathbf{r})$ were evaluated for several molecules, which exhibit different kinds of bond conjugation and electron delocalization.[52] Planar 1,3,5,7-octatetraene **1** (Figure 1a) in its all-trans configuration (C_{2h}) provides the first instance.

It serves as a representative structure for the classic π conjugation found in hydrocarbon chemistry. The negative exchange−correlation density associated with the basin of a terminal carbon

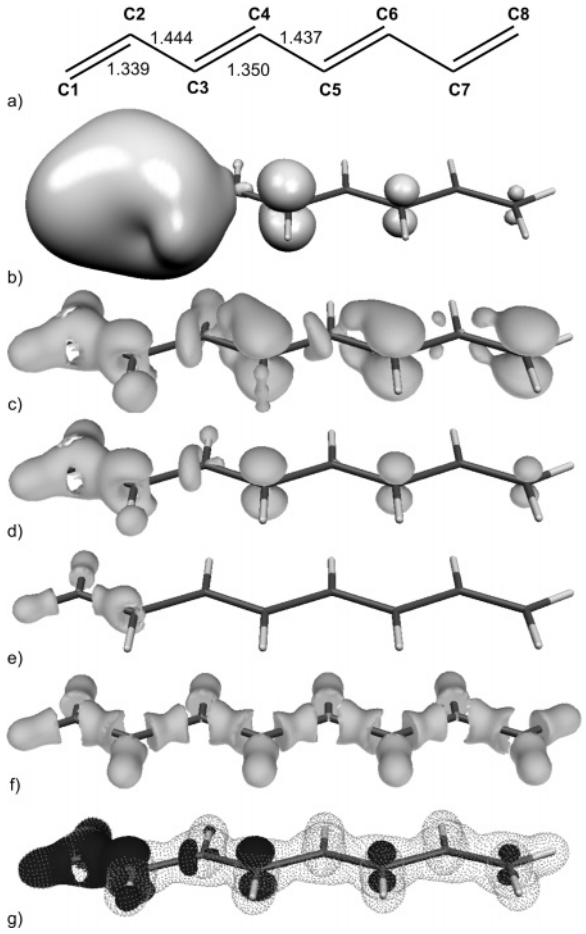

Figure 1. (a) 1,3,5,7-Octatetraene **1** (C_{2h}; C−C bond lengths in Å). (b) $X(\mathrm{C1};\mathbf{r}) = 0.001$ au. (c) $\nabla^2X(\mathrm{C1};\mathbf{r}) = -0.0001$ au. (d) $\nabla^2X(\mathrm{C1};\mathbf{r}) = -0.005$ au. (e) $\nabla^2X(\mathrm{C1};\mathbf{r}) = -0.25$ au. (f) $\nabla^2\rho(\mathbf{r}) = -0.25$ au. (g) Dotted gray surface: $\nabla^2\rho(\mathbf{r}) - \nabla^2X(\mathrm{C1};\mathbf{r}) = -0.01$ au; black surface: $\nabla^2X(\mathrm{C1};\mathbf{r}) = -0.01$ au.

atom, C1, is displayed in Figure 1b by the isosurface for $X(\mathrm{C1};\mathbf{r}) = 0.001$ au. It is evident that the electron population of C1 is delocalized mainly over its immediate vicinity, the corresponding part of the isosurface encloses C1, C2 and their hydrogen substituents and touches C3. It is difficult to discern any structure in this region, but at the more remote, even-numbered atoms C4, C6 and C8 the isosurface is dumbbell-shaped (resembling p-type atomic basis functions) and its spatial extension diminishes with increasing distance to C1. At this particular surface value, there is no indication of delocalization over the uneven-numbered carbon atoms C5 and C7. This alternating intensity of $X(\mathrm{C1};\mathbf{r})$ at atoms following each other along the chain is a consequence of the antisymmetry of the N-electron state; i.e., it is a manifestation of the Pauli exclusion principle. A comparison with Figure 1f, which displays an isosurface of the Laplacian of the electron density ($\nabla^2\rho(\mathbf{r}) = -0.25$ au), shows that the dumbbell-shaped regions of the $X(\mathrm{C1};\mathbf{r})$-surface at C4, C6 and C8 fit approximately into the space between core and valence shell charge concentrations of these atoms. This is in line with the expectation that delocalization over remote atoms will avoid regions of local charge concentration. The integrals of $X(\mathrm{C1};\mathbf{r})$ over atomic basins, i.e. the localization index or the delocalization indices times ${}^1/_2$, respectively, are given in Table 1.

The Laplacian of $X(\mathrm{C1};\mathbf{r})$ is displayed in Figure 1c−e by means of the isosurfaces for $\nabla^2X(\mathrm{C1};\mathbf{r}) = -0.0001$, -0.005 and -0.25 au, respectively. It is apparent from the first one

TABLE 1: Values of $\int_{\Omega_m} dr\, X(\Omega_n;\mathbf{r})$ for 1−10 (Reference Basin Ω_n in Italics)

1		*C1*	C2	C3	C4	C5	C6	C7	C8
		4.033	0.868	0.039	0.046	0.004	0.015	0.001	0.008
2		C1	C2	C3	C4	C5	*C6*	C7	C8
		0.013	0.003	0.047	0.040	0.872	4.029	0.003	0.002
3		*C1*	C2	C3	C4	C5	C6	C7	C8
		4.070	1.232	0.050	0.086	0.007	0.028	0.002	0.013
4		*C1*	C2	C3	C4	C5	C6	C7	C8
		3.913	0.496	0.025	0.006	0.001	0.000	0.000	0.000
5		*C1*	C2	C3	C4				
		3.947	0.693	0.037	0.052				
6		C1	C2	C3	C4	C5	C6	*C7*	C8
		0.135	0.027	0.025	0.026	0.050	0.724	3.946	0.501
6		C1	C2	C3	*C4*	C5	C6	C7	C8
		0.026	0.034	0.688	3.926	0.688	0.034	0.026	0.008
7		*S1*	N1	S2	N2	S3			
		13.182	0.646	0.062	0.064	0.213			
7		*N1*	S2	N2	S3	N3			
		6.431	0.646	0.086	0.064	0.039			
8		*C1*	C2	C3					
		4.164	0.486	0.373					
9		*Cl1*	Cl2	O1	O2				
	α	8.024	0.259	0.054	0.026				
	β	8.017	0.260	0.056	0.031				
9		Cl1	Cl2	*O1*	O2				
	α	0.054	0.026	3.709	0.347				
	β	0.056	0.031	3.068	0.480				
10		*C1*	C2	Li1					
		4.811	0.032	0.043					
10		*Li1*	Li2	C2					
		1.968	0.001	0.043					

(Figure 1c) that the fundamental structure of the delocalization originating from C1 resembles very much the classical concept of π conjugation. The surface encloses the connection lines between C1 and the directly bonded atoms, corresponding to σ delocalization (over the hydrogen atoms) and $\sigma + \pi$ delocalization (over C2). On the more remote atoms it consists mainly of two separate parts, each located on opposite sides of the molecular plane, corresponding to π delocalization. Furthermore, it extends much more between two doubly bonded atoms than between two singly bonded ones, in accord with the π system being the principal track for remote delocalization. The isosurface value of Figure 1d (−0.005 au) is appropriate for comparison with the original $X(C1;\mathbf{r})$-function (Figure 1b). The most pronounced differences concern the immediate vicinity of C1. This region now resembles the corresponding region of $\nabla^2\rho(\mathbf{r})$ in Figure 1f, with which it would be identical if no electrons from other atoms would be delocalized over C1; Figure 1e, which has the same isosurface value as the one used for $\nabla^2\rho(\mathbf{r})$ in Figure 1f (−0.25 au), demonstrates this similarity. The decrease in spatial extension of the isosurface with increasing distance from the reference basin in $X(C1;\mathbf{r})$ is also found in $\nabla^2X(C1;\mathbf{r})$, but it is much less pronounced. Figure 1g shows how $\nabla^2X(C1;\mathbf{r})$, represented by the black surface, contributes according to eq 12 to the Laplacian of the electron density, the dotted surface belongs to $\nabla^2\rho(\mathbf{r}) - \nabla^2X(C1;\mathbf{r})$.

π Delocalization along a planar chain of alternating single and double bonds will become interrupted, if the chain is twisted around a single bond by 90°. 3-Vinyl-1,3,5-hexatriene **2**, with the 3-vinyl group oriented perpendicular to the C_6 chain,[53] is a model structure for this effect (Figure 2a).

Figure 2b shows the negative exchange−correlation density associated with the terminal carbon atom C6 by the isosurface for $X(C6;\mathbf{r}) = 0.001$ au. Its structure along the planar chain, from C6 to C1, is essentially identical with the one for octatetraene **1** (cf. Figure 1b). The surface extends not over the perpendicularly oriented 3-vinyl group. This interruption of delocalization is also apparent from the integrals of $X(C6;\mathbf{r})$,

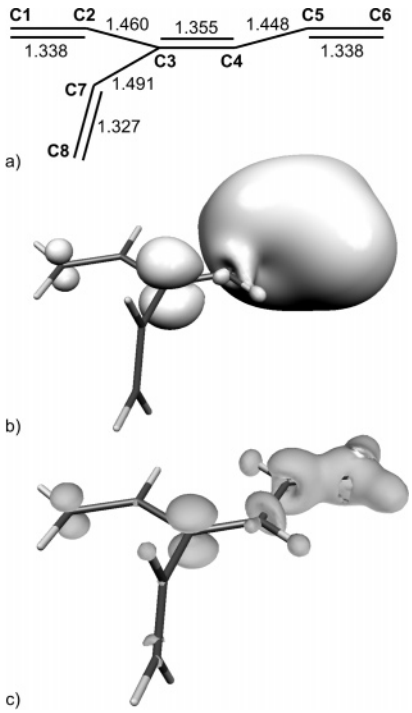

Figure 2. (a) 3-Vinyl-1,3,5-hexatriene **2** (C_1; C−C bond lengths in Å). The 3-vinyl group is oriented perpendicular to the hexatriene chain. (b) $X(C6;\mathbf{r}) = 0.001$ au. (c) $\nabla^2X(C6;\mathbf{r}) = -0.005$ au.

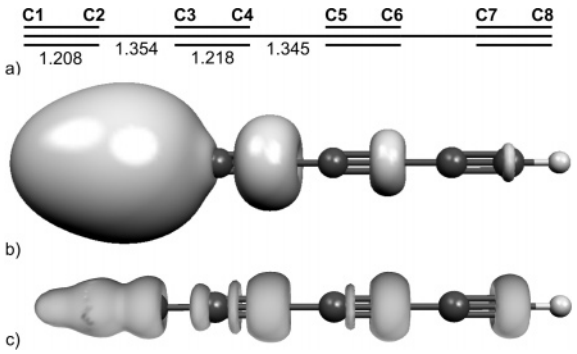

Figure 3. (a) 1,3,5,7-Octatetrayne **3** ($D_{\infty h}$; C−C bond lengths in Å). (b) $X(C1;\mathbf{r}) = 0.001$ au. (c) $\nabla^2X(C1;\mathbf{r}) = -0.0005$ au.

which are 0.013 and 0.002, respectively, for the two different terminal carbon atoms C1 and C8 (cf. Table 1). The Laplacian of $X(C6;\mathbf{r})$, which is displayed in Figure 2c by the isosurface for $\nabla^2X(C6;\mathbf{r}) = -0.005$ au, clearly preserves this quantitative difference between both parts of the chain.

For the triple bond system analogous to **1**, 1,3,5,7-octatetrayne **3** (Figure 3a), the delocalization originating from a terminal carbon atom is visualized in Figure 3b by the isosurface for $X(C1;\mathbf{r}) = 0.001$ au.

Its main features, i.e., alternating intensity and overall decreasing extension with increasing distance to the reference atom, are similar to those of **1**, but the closed parts of the surface at C4, C6 and C8 are of toroidal shape. The integrals (Table 1) indicate considerably stronger remote delocalization than in octatetraene **1**, on even-numbered atoms (C4, C6, C8) it is larger in size by a factor of 1.6−1.9. The Laplacian of $X(C1;\mathbf{r})$, displayed in Figure 3c with $\nabla^2X(C1;\mathbf{r}) = -0.0005$ au, likewise contains the toroidal regions around C4, C6 and C8. In addition, there are three[54] small tori in vicinity of, but not directly around, C3 and C5, which are the residuals of delocalization over these uneven-numbered atoms, in the case of which the Pauli principle interferes (vide supra).

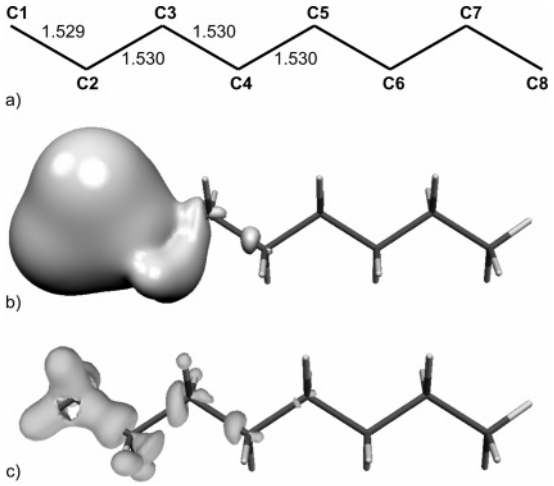

Figure 4. (a) Octane **4** (C_{2h}; C−C bond lengths in Å). (b) X(C1;**r**) = 0.001 au. (c) ∇^2X(C1;**r**) = −0.005 au.

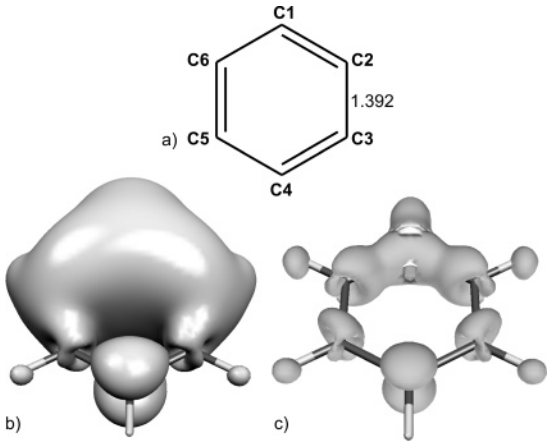

Figure 5. (a) Benzene **5** (D_{6h}; C−C bond length in Å). (b) X(C1;**r**) = 0.001 au. (c) ∇^2X(C1;**r**) = −0.005 au.

In case of the corresponding saturated compound, octane **4** (Figure 4a), one expects no pronounced delocalization along the chain.

The negative exchange−correlation density originating from the terminal carbon atom C1 is visualized in Figure 4b by the isosurface for X(C1;**r**) = 0.001 au. In contrast to the analogous surfaces for **1**−**3** it extends only until C4 and the integral over the basin of the latter (Table 1) is 7.7 times lower than the corresponding value for **1**. The Laplacian of X(C1;**r**) in Figure 4c (∇^2X(C1;**r**) = −0.005 au) preserves this limited spatial extension.

The archetypical conjugated system benzene[55] **5** (Figure 5a) resembles, as expected, octatetraene **1** in the qualitative shapes of X(C1;**r**) and its Laplacian (Figure 5b,c) but differs from it quantitatively.

In particular, the integral (Table 1) of X(C1;**r**) over the basin of the para carbon atom (C4) is 13% larger than the corresponding one in **1**.[56]

It is evident from the analysis of **1**−**5** that the structures of the negative exchange−correlation density and its Laplacian contain remarkably clear, orbital-independent information about electron delocalization, which is essentially in accord with the basic concepts of conjugation. Particularly instructive is the application of $X(\Omega_n;\mathbf{r})$ and $\nabla^2X(\Omega_n;\mathbf{r})$ in the context of less common electronic interactions, such as the phenomenon of homoconjugation. The homotropylium cation **6** is regarded as

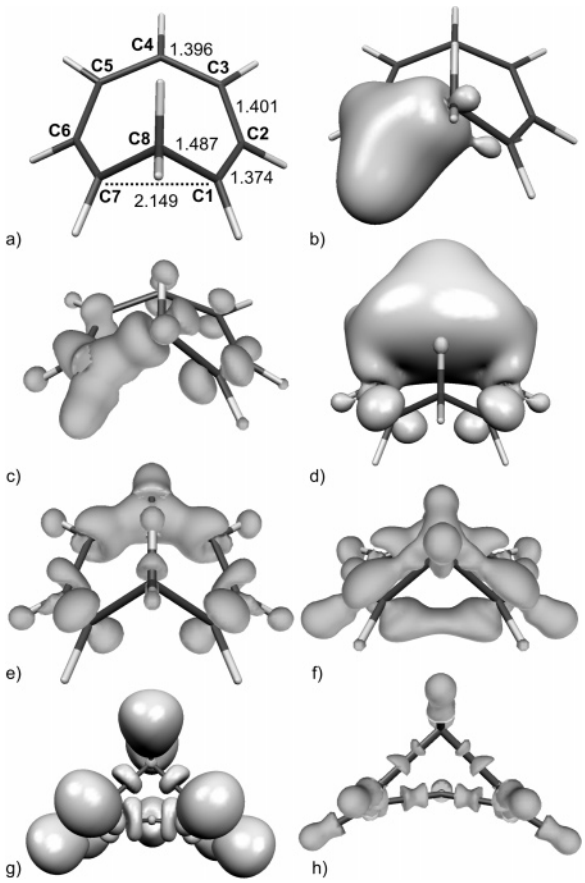

Figure 6. (a) Homotropylium cation **6** (C_s; C−C distances in Å). (b) X(C7;**r**) = 0.0145 au. (c) ∇^2X(C7;**r**) = −0.01 au. (d) X(C4;**r**) = 0.001 au. (e) ∇^2X(C4;**r**) = −0.005 au. (f) ∇^2X(C4;**r**) = −0.0005 au. (g) Electron localization function, η(**r**) = 0.80. (h) $\nabla^2\rho$(**r**) = −0.60 au.

a cyclically conjugated, homoaromatic system, based on energetic and magnetic criteria.[57,58a] Its nonplanar structure is displayed in Figure 6a.

It is assumed that homoconjugation occurs directly through the space between C1 and C7, which are separated by a methylene unit (C8). In the isosurface for X(C7;**r**) = 0.0145 au (Figure 6b) one recognizes a small droplet-shaped region that extends straight ahead (i.e., not along the detour of the bonds C7−C8 and C8−C1) in the direction of C1. The integral of X(C7;**r**) over the basin of C1 (Table 1) amounts to 0.135, i.e., the delocalization index, the number of electrons delocalized from C7 over C1 and vice versa, is 0.270.[18,19] The corresponding Laplacian in Figure 6c (∇^2X(C7;**r**) = −0.01 au) contains dumbbell-shaped regions at the remote carbon atoms C1−4 and the largest one is found at the homoconjugated C1. A striking view, with obvious similarities to the molecular orbital model of homoconjugation,[58] is obtained by choosing C4 as the reference basin. The isosurfaces for X(C4;**r**) = 0.001 au (Figure 6d) and for ∇^2X(C4;**r**) = −0.005 au (Figure 6e) show two pronounced dumbbell-shaped regions at C1 and C7, which melt together and form a single region along the presumed direction of homoconjugation upon further lowering of the magnitude value of ∇^2X(C4;**r**) (Figure 6f). Despite this *through space* delocalization associated with C1 and C7, the topological analysis of the electron density[1,2] gives no (3, −1) critical point[10] between them; i.e., there is no bonding present (this finding was termed *no bond homoaromaticity*[58]). Correspondingly, the electron localization function (Figure 6g)[59] and the Laplacian

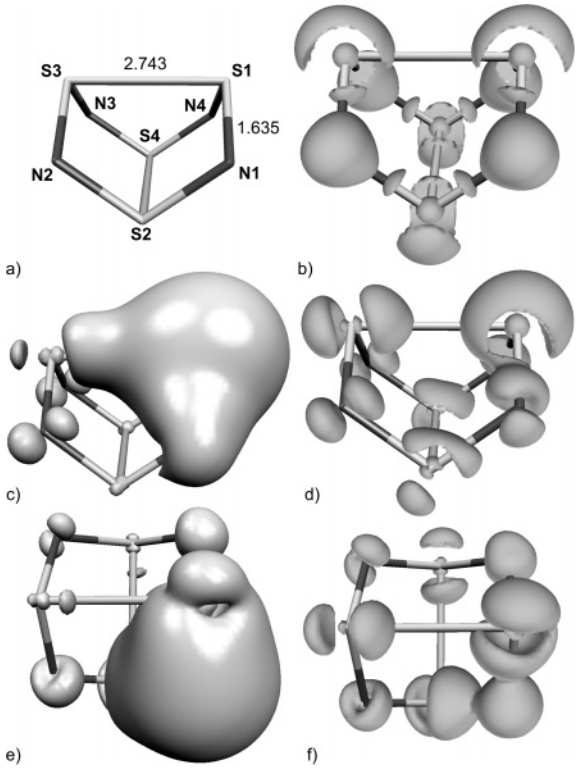

Figure 7. (a) Tetrasulfur tetranitride **7** (D_{2d}; bond lengths in Å). (b) $\nabla^2\rho(\mathbf{r}) = -0.25$ au. (c) $X(\mathrm{S1};\mathbf{r}) = 0.005$ au. (d) $\nabla^2X(\mathrm{S1};\mathbf{r}) = -0.015$ au. (e) $X(\mathrm{N1};\mathbf{r}) = 0.005$ au. (f) $\nabla^2X(\mathrm{N1};\mathbf{r}) = -0.015$ au.

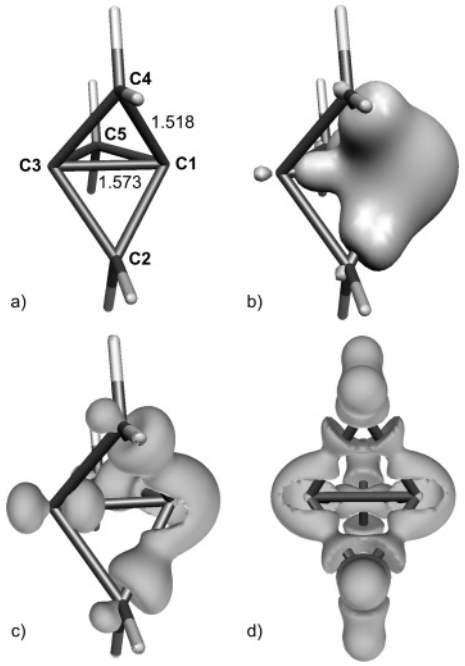

Figure 8. (a) [1.1.1]Propellane **8** (D_{3h}; C−C bond lengths in Å). (b) $X(\mathrm{C1};\mathbf{r}) = 0.05$ au. (c) $\nabla^2X(\mathrm{C1};\mathbf{r}) = -0.1$ au. (d) $\nabla^2\rho(\mathbf{r}) = -0.3$ au.

of the electron density (Figure 6h) contain no maxima between C1 and C7.[60]

Tetrasulfur tetranidride **7** (Figure 7a) can be regarded as a conjugated ring system featuring additional transannular interactions between opposite sulfur atoms: the S−N bond length is within the normal range, but the S1−S3 (S2−S4) distance (2.743 Å; experimental value: 2.60 Å[61]) is significantly larger than for usual S−S single bonds (e.g., 2.05 Å for polysulfides[62]).

Nonetheless, there are (3, −1) critical points present in $\rho(\mathbf{r})$ between such opposite sulfur atoms. The $\nabla^2\rho(\mathbf{r})$ isosurface in Figure 7b ($\nabla^2\rho(\mathbf{r}) = -0.25$ au) exhibits crescent-shaped regions in the valence shell charge concentration of the sulfur atoms. These cover both the nonbonded "lone pair" electron density and the S−S bond,[63] whereas unique separated regions are present in direction of the S−N bonds.[64] The electron population of S1 is primarily delocalized not only over the adjacent nitrogen atoms N1 and N4 but also over the opposite S3 atom, as indicated by the isosurface for $X(\mathrm{S1};\mathbf{r}) = 0.005$ au in Figure 7c (the integrals are 0.646 over N1/N4 and 0.213 over S3; cf. Table 1). This surface is almost absent at S2 and S4 (integral: 0.062), although they have nearly the same spatial distance (2.750 Å) to the reference basin (S1) like S3. As indicated by the bond critical point ($\mathbf{r}_b$) properties, the transannular S1−S3 bond ($\rho(\mathbf{r}_b) = 0.046$ au; $\nabla^2\rho(\mathbf{r}_b) = 0.038$ au; kinetic energy per electron $G(\mathbf{r}_b)/\rho(\mathbf{r}_b) = 0.387$ au) is clearly different in character from the S1−N1/N4 bonds ($\rho(\mathbf{r}_b) = 0.227$ au; $\nabla^2\rho(\mathbf{r}_b) = -0.399$ au; $G(\mathbf{r}_b)/\rho(\mathbf{r}_b) = 0.590$ au). For the S1−S3 bond, these properties are characteristic of neither typical *shared*[2] ($\rho(\mathbf{r}_b)$ large; $\nabla^2\rho(\mathbf{r}_b)$ negative; $G(\mathbf{r}_b)/\rho(\mathbf{r}_b)$ below unity) nor ionic *closed shell*[2] interactions ($\rho(\mathbf{r}_b)$ small; $\nabla^2\rho(\mathbf{r}_b)$ positive; $G(\mathbf{r}_b)/\rho(\mathbf{r}_b)$ above unity). Such differences between S−N and S−S bonding are not immediately apparent from the shape of $X(\mathrm{S1};\mathbf{r})$. The Laplacian of the latter provides a more detailed view. Figure 7d displays the isosurface for $\nabla^2X(\mathrm{S1};\mathbf{r}) = -0.015$ au. Its shape along the polar S−N bonds should be contrasted with the case of homoatomar C−C bonds in **1**−**6**. The surface between a reference C atom and a directly bonded C atom is rather uniform, but $\nabla^2X(\mathrm{S1};\mathbf{r})$ and $\nabla^2X(\mathrm{N1};\mathbf{r})$ (Figure 7f) feature a pronounced constriction between sulfur and nitrogen. This is in accord with the polar character of the S−N bond. On the other hand, $\nabla^2X(\mathrm{S1};\mathbf{r})$ exhibits even a gap along the unpolar S1−S3 bond ($\nabla^2X(\mathrm{S1};\mathbf{r}_b) = 0.004$ au). It contains, however, two rather large closed regions in front of and behind, respectively, S3. Hence, despite significant delocalization from S1 over S3 (cf. Table 1), there is, in contrast to normal *shared*[2] bonding, no local continuous concentration in the amount of delocalized electrons along the bond vector. The delocalization of electron density from the nitrogen atoms is mainly concentrated over the adjacent sulfur atoms. There are no significant transannular interactions, as indicated by the isosurfaces for $X(\mathrm{N1};\mathbf{r}) = 0.005$ au (Figure 7e) and $\nabla^2X(\mathrm{N1};\mathbf{r}) = -0.015$ au (Figure 7f). The integral of $X(\mathrm{N1};\mathbf{r})$ over the basin of the opposite N3 atom amounts to only 0.039 (Table 1) and there are no corresponding (3,−1)-critical points present in $\rho(\mathbf{r})$.

The central C1−C3 bond of [1.1.1]propellane **8** (Figure 8a) is another, rather unusual case of unpolar bonding with positive $\nabla^2\rho(\mathbf{r}_b)$.[65]

The latter amounts here to 0.100 au, although the electron density $\rho(\mathbf{r}_b)$ is quite high: with 0.185 au it approaches the range of usual C−C single bonds (cf. C1−C2: $\rho(\mathbf{r}_b) = 0.234$ au, $\nabla^2\rho(\mathbf{r}_b) = -0.384$ au; C1−C2 in **4**: $\rho(\mathbf{r}_b) = 0.239$ au, $\nabla^2\rho(\mathbf{r}_b) = -0.502$ au). The isosurface for $X(\mathrm{C1};\mathbf{r}) = 0.05$ au (Figure 8b) appears similar in shape for the two different kinds of C−C bonds and the integral over C3 is with 0.373 only 23% lower than over C2 (0.486; Table 1). The corresponding Laplacian (Figure 8c: $\nabla^2X(\mathrm{C1};\mathbf{r}) = -0.1$ au) shows, however, a clearly different structure for the central C1−C3 bond. As in the case of transannular S−S bonding in **7** (vide supra), the surface is interrupted along the bond vector, although in this case $\mathbf{r}_b$ is still located within the negative region ($\nabla^2X(\mathrm{C1};\mathbf{r}_b) = -0.022$ au). A substantial part of the $\nabla^2X(\mathrm{C1};\mathbf{r}_b)$ surface extends behind C1, away from C3. In line with this, $\nabla^2\rho(\mathbf{r})$ shows "lone pair"-

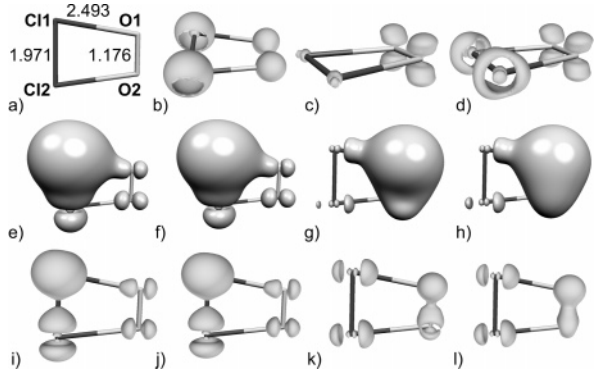

Figure 9. (a) $Cl_2O_2^+$ **9** (C_{2v}; bond lengths in Å). (b) $\nabla^2\rho(\mathbf{r}) = -0.4$ au. (c) $\nabla^2\rho^\alpha(\mathbf{r}) - \nabla^2\rho^\beta(\mathbf{r}) = -0.01$ au. (d) $\nabla^2\rho^\alpha(\mathbf{r}) - \nabla^2\rho^\beta(\mathbf{r}) = -0.003$ au. (e) $X^{\alpha(\alpha,\beta)\approx}(\mathrm{Cl1};\mathbf{r}) = 0.002$ au. (f) $X^{\beta(\beta,\alpha)\approx}(\mathrm{Cl1};\mathbf{r}) = 0.002$ au. (g) $X^{\alpha(\alpha,\beta)\approx}(\mathrm{O1};\mathbf{r}) = 0.002$ au. (h)$X^{\beta(\beta,\alpha)\approx}(\mathrm{O1};\mathbf{r}) = 0.002$ au. (i) $\nabla^2X^{\alpha(\alpha,\beta)\approx}(\mathrm{Cl1};\mathbf{r}) = -0.01$ au. (j) $\nabla^2X^{\beta(\beta,\alpha)\approx}(\mathrm{Cl1};\mathbf{r}) = -0.01$ au. (k) $\nabla^2X^{\alpha(\alpha,\beta)\approx}(\mathrm{O1};\mathbf{r}) = -0.01$ au. (l) $\nabla^2X^{\beta(\beta,\alpha)\approx}(\mathrm{O1};\mathbf{r}) = -0.01$ au.

like nonbonded regions (Figure 8d) at the bridgehead atoms C1 and C3 (the corresponding maxima in $-\nabla^2\rho(\mathbf{r})$ are located on the C1−C3 vector in a distance of 0.50 Å to the respective nuclei).

The trapezoid-shaped $Cl_2O_2^+$ cation **9**[66] (Figure 9a) is an example for a spin polarized system.

The geometry of this radical (ground state: $^2A_2$) was optimized with an unrestricted coupled cluster method [UCCSD/6-31+G(d)] and the exchange−correlation density was approximated by eq 9 ($Cl_2O_2^+$ cannot be treated with UB3LYP[66]). Its very long Cl−O bonds (2.493 Å; experimental value: 2.43 Å;[66] cf. 1.47 Å in ClO_2[67]) suggest the formal description as a weak adduct of parallel aligned [Cl_2] and [O_2] units. The charges (QTAIM) of chlorine and oxygen are similar, amounting to +0.272 and +0.228, respectively, but the spin population (the difference of α- and β-electron populations of the QTAIM basins: $N^\alpha - N^\beta$) is associated almost entirely with oxygen, where it amounts to +0.501 (chlorine: −0.001). Figure 9c shows an isosurface of the Laplacian of the spin density, $\nabla^2\rho^\alpha(\mathbf{r}) - \nabla^2\rho^\beta(\mathbf{r}) = -0.01$ au (for comparison $\nabla^2\rho(\mathbf{r})$ is displayed in Figure 9b). It extends mainly around the oxygen atoms, where it forms two dumbbells that resemble an out-of-plane π-type orbital (at surface values of lower magnitude there appear additional wheel-shaped regions around the chlorine atoms, cf. Figure 9d). Hence spin polarization in **9** occurs essentially *out* of the molecular plane, in the basins of the oxygen atoms. It follows that, if the delocalization from chlorine over the oxygen atoms takes place mainly *in* the molecular plane, there will be no pronounced difference in behavior regarding the α- and β-electron populations. The similar isosurfaces for $X^{\alpha(\alpha,\beta)\approx}(\mathrm{Cl1};\mathbf{r})$ and $X^{\beta(\beta,\alpha)\approx}(\mathrm{Cl1};\mathbf{r})$ in Figure 9e,f indicate this to be case. Correspondingly, the integrals (Table 1) are with 0.054 and 0.056, respectively, almost identical for the α- and β-reference electron populations. The same holds for the delocalization from oxygen over the essentially not-spin-polarized chlorine atoms, but it does not hold for the delocalization between two oxygen atoms. $X^{\alpha(\alpha,\beta)\approx}(\mathrm{O1};\mathbf{r})$ is expected to extend at O2 more *in* than *out* of the molecular plane, because of the predominance of α-electron density *out* of the plane. This is vaguely discernible in the isosurface of $X^{\alpha(\alpha,\beta)\approx}(\mathrm{O1};\mathbf{r})$, when compared to $X^{\beta(\beta,\alpha)\approx}(\mathrm{O1};\mathbf{r})$ (Figure 9g,h), but the integral over O2 is significantly smaller for the α- (0.347) than for the β-reference population (0.480). The Laplacians of the above functions are displayed in Figure 9i−l. It is evident that transannular delocalization occurs primarily *in* the molecular plane: the isosurfaces for

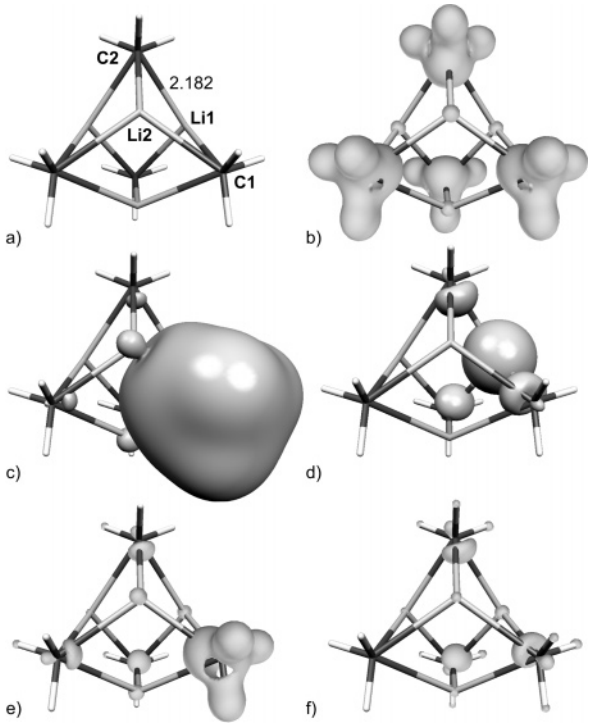

Figure 10. (a) Methyllithium tetramer **10** (T_d; bond length in Å). (b) $\nabla^2\rho(\mathbf{r}) = -0.01$ au. (c) $X(\mathrm{C1};\mathbf{r}) = 0.002$ au. (d) $X(\mathrm{Li1};\mathbf{r}) = 0.002$ au. (e) $\nabla^2X(\mathrm{C1};\mathbf{r}) = -0.01$ au. (f) $\nabla^2X(\mathrm{Li1};\mathbf{r}) = -0.01$ au.

$\nabla^2X^{\alpha(\alpha,\beta)\approx}(\mathrm{Cl1};\mathbf{r})$ and $\nabla^2X^{\beta(\beta,\alpha)\approx}(\mathrm{Cl1};\mathbf{r})$ (Figure 9i,j) resemble in-plane π-type orbitals at the oxygen atoms. The surfaces for $\nabla^2X^{\alpha(\alpha,\beta)\approx}(\mathrm{O1};\mathbf{r})$ and $\nabla\,^2X^{\beta(\beta,\alpha)\approx}(\mathrm{O1};\mathbf{r})$ in Figure 9k,l demonstrate the difference between α- and β-reference electron populations for the delocalization between the oxygen atoms: the surface for the α reference population of O1 in Figure 9k clearly avoids the space above and below O2 (where α electron density predominates), in contrast to the case of the β reference population in Figure 9l.

Tetrameric methyllithium $(LiCH_3)_4$ (**10**) (Figure 10a) provides an example for ionic bonding.[68]

Its structure is best described as a distorted heterocubane and the charges (QTAIM) of lithium, carbon and hydrogen are +0.870, −0.615 and −0.085, respectively. There are bond paths between lithium and carbon atoms (with $\rho(\mathbf{r}_b) = 0.026$ au and $\nabla^2\rho(\mathbf{r}_b) = +0.113$ au), but not between the lithium atoms themselves. The isosurface for $\nabla^2\rho(\mathbf{r}) = -0.01$ au in Figure 10b shows clearly separated regions of electron density concentration for the cations and anions. As indicated by the surface for $X(\mathrm{C1};\mathbf{r}) = 0.002$ au in Figure 10c, the electron population of the carbon atoms is mainly delocalized over the hydrogen atoms. The corresponding surface for the lithium atoms, $X(\mathrm{Li1};\mathbf{r}) = 0.002$ au in Figure 10d, is less extended and the integral over C1 (Table 1) is with 0.043 very small. The Laplacians of $X(\mathrm{C1};\mathbf{r})$ and $X(\mathrm{Li1};\mathbf{r})$ in Figure 10e,f show large gaps between anions and cations and indicate that there is no local continuous concentration in the amount of delocalized electrons along the Li−C bonds.

4. Conclusions

The structure of $\nabla^2_{\langle\mathbf{r}_2\rangle}X(\mathbf{r}_1,\mathbf{r}_2)$ contains detailed information about the fundamental shape of electron delocalization in real space. Integration of the reference coordinate $\mathbf{r}_1$ over an atomic basin Ω_n, which leads to the function $\nabla^2X(\Omega_n;\mathbf{r})$, is a particularly useful way of its practical application. The qualitative investiga-

tion of $\nabla^2 X(\Omega_n;\mathbf{r})$, e.g., by means of isosurface plots as above, reveals many relevant spatial properties of electron delocalization in molecules. $\nabla^2 X(\Omega_n;\mathbf{r})$ is advantageously used together with $X(\Omega_n;\mathbf{r})$ (the latter, for example, in integrated form as delocalization indices[18,19,25]), which provides quantitative information. It should be kept in mind that the actual shape of delocalization is given by $X(\Omega_n;\mathbf{r})$. Its Laplacian $\nabla^2 X(\Omega_n;\mathbf{r})$ determines local concentrations within $X(\Omega_n;\mathbf{r})$ and is hence better suited for the analysis of its basic structure. In this sense, one may regard plots of $\nabla^2 X(\Omega_n;\mathbf{r})$ as representations of a fictitious scaffolding, along which the actual amount of delocalized electrons spreads in space.

Supporting Information Available: Cartesian coordinates of the calculated structures **1**−**10**. This material is available free of charge via the Internet at http://pubs.acs.org.

References and Notes

(1) Bader, R. F. W. *Atoms in Molecules − A Quantum Theory*; Oxford University Press: Oxford, U.K., 1990.

(2) Bader, R. F. W. *Chem. Rev.* **1991**, *91*, 893.

(3) Bader, R. F. W.; Heard, G. L. *J. Chem. Phys.* **1999**, *111*, 8789.

(4) Gillespie, R. J.; Bayles, D.; Platts, J.; Heard, G. L.; Bader, R. F. W. *J. Phys. Chem. A* **1998**, *102*, 3407.

(5) Bader, R. F. W.; Johnson, S.; Tang, T.-H., Popelier, P. L. A. *J. Phys. Chem.* **1996**, *100*, 15398.

(6) Malcolm, N. O. J.; Popelier, P. L. A. *Faraday Discuss.* **2003**, *124*, 353.

(7) Becke, A. D.; Edgecombe, K. E. *J. Chem. Phys.* **1990**, *92*, 5397.

(8) Noury, S.; Colonna, F.; Savin, A.; Silvi, B. *J. Mol. Struct.* **1998**, *450*, 59.

(9) Savin, A.; Nesper, R.; Wengert; S.; Fässler, T. F. *Angew. Chem., Int. Ed. Engl*. **1997**, *36*, 1808.

(10) Bader, R. F. W. *J. Phys. Chem. A* **1998**, *102*, 7314.

(11) Silvi, B. *J. Phys. Chem. A* **2003**, *107*, 3081.

(12) Bader, R. F. W.; Streitwieser, A.; Neuhaus, A.; Laidig, K. E.; Speers, P. *J. Am. Chem. Soc.* **1996**, *118*, 4959.

(13) Lewis, G. N. *J. Am. Chem. Soc.* **1916**, *38*, 762.

(14) Löwdin, P.-O. *Phys. Rev.* **1955**, *97*, 1474.

(15) McWeeny, R. *Rev. Mod. Phys.* **1960**, *32*, 335.

(16) Buijse, M. A.; Baerends, E. J. *Mol. Phys.* **2002**, *100*, 401.

(17) $\Gamma(1,2)$ is also frequently normalized to $N(N-1)$; i.e., the factor of $^1/_2$ in eqs 1 and 2 is omitted.[15,16] In this work the normalization defined in ref 14 is used.

(18) Fradera, X.; Austen, M. A.; Bader, R. F. W. *J. Phys. Chem. A* **1999**, *103*, 304.

(19) Fradera, X.; Poater, J.; Simon, S.; Duran, M.; Solà, M. *Theor. Chem. Acc.* **2002**, *108*, 214.

(20) Fradera, X.; Solá, M. *J. Comput. Chem.* **2002**, *23*, 1347.

(21) Wang, Y.-G.; Matta, C.; Werstiuk, N. H. *J. Comput. Chem.* **2003**, *24*, 1720.

(22) Rincón, L.; Alvarellos, J. E.; Almeida, R. *J. Chem. Phys.* **2005**, *122*, 214104.

(23) Chestnut, D. B. *Chem. Phys.* **2001**, *271*, 9.

(24) Matta, C. F.; Hernández-Trujillo, J.; Bader, R. F. W. *J. Phys. Chem. A* **2002**, *106*, 7369.

(25) Ponec, R.; Cooper, D. L. *J. Mol. Struct. (THEOCHEM)* **2005**, *727*, 133.

(26) Bochicchio, R.; Ponec, R.; Lain, L.; Torre, A. *J. Phys. Chem. A* **2000**, *104*, 9130.

(27) Ponec, R. *J. Math. Chem.* **1997**, *21*, 323.

(28) Ponec, R. *J. Math. Chem.* **1998**, *23*, 85.

(29) Fulton, R. L. *J. Phys. Chem.* **1993**, *97*, 7516.

(30) Fulton, R. L.; Perhacs, P. *J. Phys. Chem. A* **1998**, *102*, 8989.

(31) Fulton, R. L. *J. Phys. Chem. A* **2004**, *108*, 11691.

(32) Becke, A. D. *J. Chem. Phys.* **1997**, *107*, 8554.

(33) Becke, A. D. *J. Chem. Phys.* **1996**, *104*, 1040.

(34) Becke, A. D. *J. Chem. Phys.* **1993**, *98*, 5648.

(35) Lee, C.; Yang, W.; Parr, R. G. *Phys. Rev. B* **1988**, *37*, 785.

(36) Kar, T.; Ángyán, J. G.; Sannigrahi, A. B. *J. Phys. Chem. A* **2000**, *104*, 9953.

(37) Cortés-Guzmán, F.; Bader, R. F. W. *Coord. Chem. Rev.* **2005**, *249*, 633.

(38) Fradera, X.; Duran, M.; Mestres, J. *J. Comput. Chem.* **2000**, *21*, 1361.

(39) In a previous publication (Geier, J.; Rüegger, H.; Grützmacher, H. *Dalton Trans.* **2006**, 129) the name *atomic exchange density* was used for $-\Gamma_{XC}(\Omega_n;\mathbf{r})$ and was denoted as $\Gamma_{XC[\Omega]}(\mathbf{r})$. Cf. also ref 38.

(40) Ponec, R.; Yuzhakov, G.; Cooper, D. L. *Theor. Chem. Acc.* **2004**, *112*, 419.

(41) Ponec, R.; Yuzhakov, G.; Sundberg, M. R. *J. Comput. Chem.* **2005**, *26*, 447.

(42) Ponec, R.; Yuzhakov, G.; Gironés, X.; Frenking, G. *Organometallics* **2004**, *23*, 1790.

(43) Ponec, R.; Yuzhakov, G.; Carbó-Dorca, R. *J. Comput. Chem.* **2003**, *24*, 1829.

(44) Frisch, M. J.; Trucks, G. W.; Schlegel, H. B.; Scuseria, G. E.; Robb, M. A.; Cheeseman, J. R.; Montgomery, J. A., Jr.; Vreven, T.; Kudin, K. N.; Burant, J. C.; Millam, J. M.; Iyengar, S. S.; Tomasi, J.; Barone, V.; Mennucci, B.; Cossi, M.; Scalmani, G.; Rega, N.; Petersson, G. A.; Nakatsuji, H.; Hada, M.; Ehara, M.; Toyota, K.; Fukuda, R.; Hasegawa, J.; Ishida, M.; Nakajima, T.; Honda, Y.; Kitao, O.; Nakai, H.; Klene, M.; Li, X.; Knox, J. E.; Hratchian, H. P.; Cross, J. B.; Bakken, V.; Adamo, C.; Jaramillo, J.; Gomperts, R.; Stratmann, R. E.; Yazyev, O.; Austin, A. J.; Cammi, R.; Pomelli, C.; Ochterski, J. W.; Ayala, P. Y.; Morokuma, K.; Voth, G. A.; Salvador, P.; Dannenberg, J. J.; Zakrzewski, V. G.; Dapprich, S.; Daniels, A. D.; Strain, M. C.; Farkas, O.; Malick, D. K.; Rabuck, A. D.; Raghavachari, K.; Foresman, J. B.; Ortiz, J. V.; Cui, Q.; Baboul, A. G.; Clifford, S.; Cioslowski, J.; Stefanov, B. B.; Liu, G.; Liashenko, A.; Piskorz, P.; Komaromi, I.; Martin, R. L.; Fox, D. J.; Keith, T.; Al-Laham, M. A.; Peng, C. Y.; Nanayakkara, A.; Challacombe, M.; Gill, P. M. W.; Johnson, B.; Chen, W.; Wong, M. W.; Gonzalez, C.; Pople, J. A. *Gaussian 03*, revision B.04; Gaussian, Inc.: Wallingford, CT, 2004.

(45) Bauernschmitt, R.; Ahlrichs, R. *J. Chem. Phys.* **1996**, *104*, 9047.

(46) Purvis, G. D., III; Bartlett, R. J. *J. Chem. Phys.* **1982**, *76*, 1910.

(47) *AIM2000*, version 2.0: Biegler-König, F.; Schönbohm, J.; Bayles, D. *J. Comput. Chem.* **2001**, *22*, 545; http://gauss.fh-bielefeld.de/aim2000.

(48) The source code or a precompiled version (Linux) is available upon request from the author.

(49) *Molekel*, version 4.3. Flükiger, P.; Lüthi, H. P.; Portmann, S.; Weber, J.; Swiss Center for Scientific Computing, Manno (Switzerland), 2000−2002.

(50) Portmann, S.; Lüthi, H. P. *Chimia* **2000**, *54*, 766.

(51) Noury, S.; Krokidis, X.; Fuster, F.; Silvi, B.; University P. M. Curie, Paris, **1997**: Noury, S.; Krokidis, X.; Fuster, F.; Silvi, B. *Comput. Chem.* **1999**, *23*, 597.

(52) Recent reviews concerned with the investigation of electron delocalization by various means are: (a) Poater, J.; Duran, M.; Solá, M.; Silvi, B. *Chem. Rev.* **2005**, *105*, 3911. (b) Merino, G.; Vela, A.; Heine, T. *Chem. Rev.* **2005**, *105*, 3812.

(53) This conformation is not a minimum; there is one negative *Hessian* eigenvalue.

(54) Isosurfaces for smaller magnitude values of $\nabla^2 X(C1;\mathbf{r})$ contain an additional torus behind C7.

(55) A recent publication concerned with the origin of its aromaticity is: Kovaćević, B.; Barić, D.; Maksić, Z.; Müller, T. *ChemPhysChem* **2004**, *5*, 1352.

(56) A measure of aromaticity, which is derived from the integration of the exchange−correlation density over para-related basins, was proposed recently: Poater, J.; Fradera, X.; Duran, M.; Solà, M. *Chem. Eur. J.* **2003**, *9*, 400.

(57) Williams, R. V. *Chem. Rev.* **2001**, *101*, 1185.

(58) (a) Cremer, D.; Reichel, F.; Kraka, E. *J. Am. Chem. Soc.* **1991**, *113*, 9459. (b) Szabo, K. J.; Kraka, E.; Cremer, D. *J. Org. Chem.* **1996**, *61*, 2788.

(59) Lepetit, C.; Silvi, B.; Chauvin, R. *J. Phys. Chem. A* **2003**, *107*, 464.

(60) Probably one might detect an interaction between C1 and C7 by means of the coupling energy density (CED) and the coupling electron deformation density (CDD), which are derived from indirect nuclear spin−spin coupling, or by the anisotropy of the induced current density (ACID). CED/CDD: Malkina, O. L.; Malkin, V. G. *Angew. Chem.* **2003**, *115*, 4471; *Int. Ed.* **2003**, *42*, 4335. ACID: Geuenich D.; Hess, K.; Köhler, F.; Herges, R. *Chem. Rev.* **2005**, *105*, 3758.

(61) Scherer, W.; Spiegler, M.; Pedersen, B.; Tafipolsky, M.; Hieringer, W.; Reinhard, B.; Downs, A. J.; McGrady, G. S. *ChemComm* **2000**, 635.

(62) Allen, F. H.; Kennard, O.; Watson, D. G.; Brammer, L.; Orpen, A. G. *J. Chem. Soc., Perkin Trans. 2*, **1987**, *12*, S1.

(63) There is no splitting of this region upon increasing the magnitude of the isosurface value. It contains only one maximum, which is located outside the cage in 0.68 Å distance from the sulfur atom.

(64) A corresponding region, which is not apparent at this isosurface value, exists in the valence shell charge concentration of the nitrogen atoms.

(65) The topological analysis of the experimentally determined electron density of a [1.1.1]propellane derivative is described in: Messerschmidt, M.; Scheins, S.; Grubert, L.; Pätzel, M.; Szeimies, G.; Paulmann, C.; Luger, P. *Angew. Chem.* **2005**, *44*, 3925; *Int. Ed.* **2005**, *44*, 3925.

(66) Drews, T.; Koch, W.; Seppelt, K. *J. Am. Chem. Soc.* **1999**, *121*, 4379.

(67) Rehr, A.; Jansen, M. *Inorg. Chem.* **1992**, *31*, 4740.

(68) The bonding between lithium and carbon in alkyllithium compounds is characterized as an ionic interaction on grounds of the following. (a) QTAIM charges and bond critical point properties: Scherer, W.; Sirsch, P.; Shorokhov, D.; McGrady, G. S.; Mason, S. A.; Gardiner, M. G. *Chem. Eur. J.* **2002**, *8*, 2324. (b) The electron localization function: Fressigné, C.; Maddaluno, J.; Giessner-Prettre, C.; Silvi, B. *J. Org. Chem.* **2001**, *66*, 6476. (c) Natural population analysis: Kaufmann, E.; Raghavachari, K.; Reed, A. E.; Schleyer, P. von R. *Organometallics* **1988**, *7*, 1597. Hirshfeld and VDD charges indicate much less ionic character: Guerra, C. F.; Handgraaf, J.-W.; Baerends, E. J.; Bickelhaupt, M. F. *J. Comput. Chem.* **2004**, *25*, 189.